B cell αv integrin regulates germinal center derived lung-resident IgA B cell responses following influenza virus infection.

Andrea Montiel-Armendariz[1]†, Kelsey Roe[1]†, Jonathan Lagos-Orellana[1], Laura Veronica Martinez-Castro[1], Adam Lacy-Hulbert[2] and Mridu Acharya[1,3]*

[1]Seattle Children's Research Institute, Seattle, WA

[2]Benaroya Research Institute, Seattle, WA

[3]Department of Pediatrics, University of Washington, Seattle, WA

†AMA and KR contributed equally to the manuscript.

*Corresponding author:

Mridu Acharya, Seattle Children's Research Institute, Seattle, WA, USA

Telephone: (206) 884 2349

Mridu.acharya@seattlechildrens.org

Abstract

Emerging studies have highlighted the importance of tissue-resident B cells in the lungs, for protective immunity against respiratory viruses. However, the mechanisms controlling generation and maintenance of such tissue-resident B cells at respiratory sites remain obscure. We have previously shown that αv integrins limit B cell responses to antigens containing Toll-like receptor ligands, and that deletion of B cell αv integrins, in mice, enhances germinal center (GC)-derived long-lived B cell responses after systemic immunization with viral antigens. Here we investigated whether αv also regulates B cell responses at the respiratory tract during viral infection. Our data show that αv integrin restricts tissue-resident B cell responses in the airway, and that deletion of B cell αv promotes generation of lung-resident IgA B cell responses following influenza A virus (IAV) infection. Investigating the mechanism for this, we found that loss of B cell αv, promotes persistence of GC reactions locally in the lungs, which leads to increases in lung-resident IgA+ memory B cells, cross-reactive to antigenic variants. Thus, these studies reveal how IgA B cells are maintained in the lungs and point to a new strategy to improve the durability of lung-resident IgA B cell responses for IAV vaccine efficacy.

Abbreviations: *GC: germinal center; IAV: Influenza A Virus; TLR: Toll-like receptor; SHM: somatic hyper mutation; medLN: Mediastinal Lymph Node; cKO: αv conditional knockout mice; HA: Hemagglutinin; iBALT: inducible bronchus-associated lymphoid tissues.*

Introduction

B cells are crucial in mediating immune responses against rapidly mutating pathogens, such as mucosal respiratory viruses, human immunodeficiency virus (HIV), and malaria, as they can generate antibodies of varying affinities and reactivities, able to target mutation induced antigenic variants. Furthermore, long-lived plasma cells and memory B cells can provide long-term protection against re-infection from the same pathogen or antigenic variants of the pathogen. While these features of B cell responses have been appreciated in the context of systemic immune responses, recent studies are also revealing the importance of pulmonary B cell responses against respiratory viruses. For example, antigen-specific lung-resident memory B cells elicited by influenza virus infection have been shown to be critical for protection against secondary infection[1]. Another study showed that these lung-resident memory B cells are of IgA isotype and differentiate to produce the mucosal immunoglobulin, IgA, which possesses unique characteristics for mucosal immunity[2]. However, despite multiple evidence showing the importance of lung-resident B cells in protective immune response at the respiratory tract, it is still not clear how they develop, are maintained, and how to generate equivalent responses through vaccination.

Identification of new mechanisms that regulate pulmonary B cell responses could allow us to develop strategies to promote these responses. In previous studies, we described a new mechanism of regulation of B cell responses by the αv family of integrins. αv integrins are a family of integrins with diverse roles in multiple immune cell populations, such as dendritic cells, macrophages, T cells, and B cells[3-10]. We described a new function for αv integrins in regulating B cell responses to Toll-like receptor (TLR) ligands and TLR ligand containing antigens, via regulation of intracellular trafficking events[11]. Although αv forms 5 different integrin heterodimers, our studies indicate that this TLR related role is mediated primarily by the αvβ3 heterodimer[11, 12]. TLR ligands are integral components of both self-derived and pathogen derived antigens and this regulatory role of αv integrin limits self-reactive B cell responses in the context of autoimmunity. Therefore, loss of B cell αv integrins accelerates development of autoimmunity in mouse models of TLR ligand driven autoimmunity[13]. However, loss of αv from B cells is also beneficial in the context of immune responses to viral antigens. Our studies showed that loss of B cell αv from mice leads to increases in germinal center (GC) derived antibody response, memory B cells and long-lived plasma cells, after systemic immunization with TLR ligand containing virus like particles. More importantly, loss of B cell αv led to increases in somatic hyper mutation (SHM) of antibodies, relevant for changing the affinity and breadth of reactivity of antibodies. These changes in B cell responses were particularly beneficial for development of protective immunity against influenza virus, as mice lacking B cell αv integrins developed more cross-reactive antibodies after systemic immunization with a single strain. B cell specific αv knockout mice also showed better protection during infection with influenza virus[14]. Based on these findings, we investigated whether the role of αv in regulating B cell TLR responses could also be relevant to regulate pulmonary B cell responses during infection with respiratory viruses.

Here we show that αv integrins play an important role in regulating tissue-resident B cell responses in the lungs. Our data show that B cell αv integrin restricts development of lung-resident IgA+ B cells after viral infection, through its B cell intrinsic role on processing of TLR signaling. Loss of B cell αv, leads to persistence of GC reactions occurring in the lungs and this results in increases in IgA+ GC and memory B cells that are cross-reactive to antigenic variants of infecting virus. These data firstly clarify that IgA B cell responses can be generated through GC reactions occurring in the lungs and secondly, they show that

blockade of B cell αv provides a new strategy to promote long-lived GC reactions in tissue sites such as the lungs for durable immunity against respiratory viruses.

Results

Generation of cross-reactive B cell responses in the lungs is regulated by B cell αv integrin.

Our previous studies showed that loss of B cell αv integrins led to increased protection of mice after infection with influenza virus and we wanted to understand whether this was because of the ability of αv integrins to regulate systemic B cell responses, as we had shown previously or whether αv also had a role in regulating tissue resident B cell responses. To determine whether αv integrins regulate B cell responses in tissue, we investigated the generation of IAV-specific B cells in the lung during infection. B cell specific αv conditional knockout mice (referred to as cKO mice) and matched controls were infected with a sub-lethal dose of H1N1 PR8 IAV, and lungs and mediastinal LNs (medLNs) harvested 14 days later for analysis of B cell response (**Figure 1A**). We used ELISPOT assay to first identify overall changes in antigen specific lung B cells. ELISPOT data revealed that lungs from cKO mice showed increase in influenza hemagglutinin (HA) -specific IgG-producing B cells compared to the lungs from control mice (**Figure 1B**). Notably, while this increase was seen with IgG producing cells reactive to HA from H1N1 PR8 strain used for infection, the increase in cKO lungs was more pronounced for cells producing IgG reactive to HA from the pandemic H1N1 California2009 (Cal09) strain (**Figure 1B**). This suggested that similar to what we saw with systemic immunization, loss of B cell αv promotes generation of antigen specific and cross-reactive B cells after influenza infection. IAV infection also induced anti-HA IgG-producing B cells, in the medLN (**Figure 1C**). However, in the medLN, we observed no differences between control and cKO mice, in generation of IgG producing cells that recognize either PR8-HA or Cal09-HA (**Figure 1C**), indicating deletion of αv from B cells increases B cell responses in the lungs after infection.

To identify B cell subpopulations associated with increased B cell responses in the lungs of cKO mice, we injected mice with an α-CD45 antibody in the retro-orbital cavity five minutes prior to euthanasia and used flow cytometry to identify lung-resident cells that were in the lung parenchyma (gating strategy on **Supp Fig 1**) (lung-resident cells identified as being i.v. $CD45^-$, **Supp Fig 2A**). Total numbers of lung-resident B cells were similar in control and cKO mice after PR8 infection indicating there were no major changes in recruitment of B cells to the lungs after infection (**Figure 1D**). Analysis of major B cell subpopulations including GC and memory B cells, indicated slight increases in lung-resident B cells with GC phenotype (Fas^+, PNA^+) in the lungs from cKO mice. As we have seen previously in the peyer's patches[14] we found some basal increase in lung-resident B cells with GC phenotype in the cKO mice, which was further increased with infection (**Figure 1E**). To analyze changes in influenza specific B cells within these compartments, we used linear HA tetramers that could identify by flow cytometry both HA-PR8 reactive and HA-Cal09 reactive B cells after infection with PR8 (**Sup Figure 2B**). cKO and control mice showed similar numbers of lung-resident PR8-HA-binding GC B cells after infection. There was a slight increase in lung-resident PR8-HA binding switched memory B cells (Sw Mem B cells) in the cKO mice (**Sup Figure 2C**). However, the cKO mice showed significantly more Cal09-HA-binding lung-resident GC B cells as well as Cal09-HA-binding class-switched lung-resident switched memory B cells (**Figure 1F**) after infection. We saw no difference in either PR8-HA or Cal09-HA-binding lung-resident IgM^+ Memory B cells in between cKO and control mice (**Figure 1F and Sup Figure 2C**), indicating the role of αv in modulating cross-reactive, lung-resident B cells is related to GC derived B cells. Additionally, we identified PR8-HA or Cal-09 -HA specific GC and memory B cells induced by infection in the medLN; however, we did not observe

differences in number or relative frequency of these cells from medLN in cKO mice compared with controls (**Sup Figure 3**). Previous studies have indicated that lung-resident B cell responses are more geared towards cross-reactive B cell responses[15] and our studies show that B cell αv integrin regulates generation of such cross-reactive B cells specifically in the lungs following infection.

Loss of B cell αv integrin increases the proportion of IgA$^+$ cells in the lungs of influenza infected mice.

Multiple studies have reported that the generation of IgA-class-switched B cells is critical for effective immunity against respiratory viruses. However, it is still not clear whether IgA B cells are generated and maintained in the lungs and the mechanisms regulating IgA B cell responses in the lungs are also not known. Based on our findings that αv integrins regulate lung B cell responses, we asked whether B cell αv integrin could regulate the induction of lung IgA B cells, following influenza infection. At day 14 post infection, both cKO and control mice generated HA-reactive IgA-producing cells, as seen by ELISPOT analysis (**Figure 2A**). Interestingly, similar to our findings with IgG, lungs from cKO mice showed significantly higher numbers of IgA-producing cells that recognized HA from Cal09 strain compared with controls (**Figure 2A**). This suggests that αv regulates generation of cross-reactive IgA B in the lungs following infection.

To understand how loss of B cell αv was leading to increases in IgA producing cells, we analyzed the phenotype of IgA+ cells by flow cytometry. Few IgA-switched cells were present prior to infection in lungs of cKO or control mice. Following infection, IgA-class switched B cells were induced in the GC, PC and switched memory B cell compartments in the control mice. Strikingly, IgA+ cells in these compartments were all expanded by approximately 2-fold in cKO mice compared with controls **(Figure 2 B-G**). This indicated that loss of αv was leading to GC dependent increases in IgA B cell responses. To understand whether the increased IgA+ cells in the cKO lungs were mainly tissue localized cells, we also analyzed circulating CD45$^+$ cells found in the lungs. These data confirmed that the increase in IgA+ cells in the cKO mice was specific to lung-resident cells i.v CD45$^-$ cells (**Figures 2C, E and G**). Moreover, analysis of both i.v. CD45$^-$ and i.v. CD45$^+$ cells found in the lungs, highlighted that while IgA negative B cells were distributed in both the circulating and lung-resident compartments, majority of the IgA+ GC and memory B cells were lung-resident (**Figure 2C** and **Sup Figure 4A-E**). Furthermore, comparison of IgA+ GC cells in the lungs versus medLN showed that IgA+ GC cells were increased in the lungs compared to medLNs in both control and cKO mice and this increase was further enhanced in the cKO lungs. (**Sup Figure 4F**). Moreover, comparison of IgA and IgG HA-specific secreting cells in the lungs and medLN also confirmed that IgA secreting cells were found predominantly in the lungs and not in the lymph nodes and the increases seen in the cKO mice were mainly in the lungs (**Sup Figure 4G-H**). Thus, these data reveal that IgA isotype B cells are primarily lung-resident and are related to GC derived long-lived B cell responses in the lungs. αv integrin on B cells modulates the generation of these lung-resident IgA isotype B cells, such that loss of αv leads to increase in infection induced GC derived IgA+ B cells in the lungs.

Loss of B cell αv integrin promotes infection induced GC reactions locally in the lungs.

To further investigate whether the loss of B cell αv was leading to increases in lung-resident IgA B cells, directly through immune reactions occurring in the lungs, we turned to confocal microscopy. Generation of inducible bronchus-associated lymphoid tissues (iBALT) in the lungs after influenza infection, has been previously described and these structures are known to be associated with GC cells[16, 17]. Therefore, we

investigated whether the increased lung-resident B cell responses in the cKO mice was associated with iBALT-GC structures in the lungs.

We isolated lungs from mice, at day 16 after infection, and performed confocal analysis of lung sections (**Figure 3A**). Confirming our flow cytometry data, we found that the cKO mice lungs had more IgA+ cells, compared to the control lungs after infection (**Figure 3B**). Next, we wanted to know if the cKO mice had an increased number of iBALT- GCs, or if the GC structure would be bigger when compared to the control lungs after infection. We used GL7 to mark GC cells (**Supp Fig 5**) and CD19 or B220 staining to identify B cells. We identified regions where GL7+ B cells clustered together and defined these as iBALT areas with GC cells. These iBALT regions with GC B cells were close to airway structures in lungs from both genotypes. However, lungs from control mice showed much smaller clusters of GC cells while the cKO mice showed bigger iBALT areas with large distinct clusters of GC cells. (**Figure 3C and D**). Quantification of either the area of iBALT-GCs or of GL7 staining within the iBALT regions both confirmed that the clusters of GC cells were larger in the lungs from cKO mice, compared to the lungs of the control mice (**Figure 3E-F)**. The kinetics of GC reactions in the lung tissue is known to be slightly delayed compared to the lymph nodes with GC structures arising in the lungs around day 21[15, 18] . These microscopy data indicate that loss of B cell αv integrin leads to earlier occurrence of GC reactions directly in the lungs, leading to generation of larger iBALT structures at day 16.

Finally, to assess whether these lung GC reactions lead to generation of IgA B cells, we quantified the area of IgA+ cells within the iBALT-GC areas and also calculated the overlap of IgA and GL7 signal within these areas (**Figure 3D and G-H**). The area of IgA+ cells within the iBALT was significantly increased in cKO lungs compared to the control group (**Figure 3G**). Lungs from cKO mice also showed a significant increase in IgA+ GL7+ cells within the iBALT areas compared to the control lungs (**Figure 3H**). These data thus establish that IgA + B cells arise from GC reactions in the lungs and loss of B cell αv promotes the generation of GC reactions the lungs which leads to the increase in IgA+ B cells in the lungs of these mice after infection.

Loss of B cell αv integrin promotes sustenance of lung-resident IgA memory B cells through persistence of GC reactions in the lungs.

We were curious whether these early increases in lung-resident GC B cells, seen in the cKO mice could sustain B cell responses over time, thus we measured the proportions of lung-resident GC and memory B cell responses at day 35 post PR8 IAV infection (**Figure 4A**). In control mice we identified a very small proportion of lung-resident GC B cells at day 35 after infection, by flow cytometry. However, these lung-resident GC B cells were present at significantly higher percentage in cKO mice, at this time point after infection (**Figure 4B**). Within this GC compartment, we were able to identify a small percentage of IgA-expressing B cells which were mainly present in the cKO lungs and not in the controls (**Figure 4B**). cKO mice also had a significant increase in the percentage of lung-resident memory B cells compared with controls (**Figure 4C**). Within the memory B cell compartment the cKO mice had highly elevated numbers of IgA+ Mem B cells, whereas in control mice, these had returned to levels similar to the uninfected mice (**Figure 4C**). The overall frequency of plasma cells was also low at this time point; however, we still detected a slight increase in percentage of IgA+ PCs in the cKO mice, compared to the controls (**Figure 4D**).

To confirm whether loss of αv promotes changes in kinetics of GC and memory B cells in the lungs of mice after infection, we compared the data from lungs harvested at day 14 or day 35 after infection, analyzing

numbers of cells per lung. This confirmed a sustained increase in lung-resident GC B cells over time in the lungs of cKO mice (**Figure 4E**). While the numbers of GC B cells declined in both control and cKO lungs from day 14 to 35 after infection, this decline was less drastic in the cKO lungs, and the lungs from cKO mice showed significant increase in numbers of GC B cells compared to lungs from control mice at day 35 post infection. On the other hand, the IgA+ memory B cells showed a sharp increase in the cKO lungs from day 14 to 35 after infection while the control mice showed only a small induction of IgA+ memory B cells at both time points after infection (**Figure 4E**). These data indicate that the persistent increase in GC cells in the cKO lungs leads to sustained output of IgA+ memory B cells.

As the proportion of HA-specific cells was lower at this late time point than at day 14 following infection, we made use of conformationally intact HA tetramers [19, 20]rather than the linear HA probes used in **Figure 1**, to more sensitively identify HA-specific B cells in this analysis. We verified that these tetramers could be used to identify antigen-specific cells by flow cytometry (**Sup Figure 6A**). These data showed that, antigen specific (PR8-HA+) or cross-reactive (Cal09-HA+) GC B cells were still present in cKO mice at this time point, whereas none could be detected in controls (**Figure 4F**). We also found a small percentage of PR8-HA specific Mem B cells and IgA MemB cells, present only in the cKO mice (**Sup Figure 6B**) and there was a very low percentage of Cal09-HA+ Mem B cells in mice of both genotype at this time point (**Sup Figure 6C**).

To further understand the characteristics of the small number of antigen-specific cells expanded in the cKO lungs, we performed a cluster analysis (**Figure 4G**). Using the Cytofkit package from Biocunductor[21]**,** we performed a PhenoGraph clustering analysis, based on the makers used for flow cytometry staining and identified 11 statistically distinct clusters within the HA-reactive lung-resident IgD^- activated B cell compartment. We found 4 of these clusters (11, 4, 2 and 7) had a higher frequency of cells in the cKO mice, compared to controls. Interestingly, all of these 4 clusters showed both higher IgA expression and increased staining for Cal09-HA, compared to other clusters (**Figure 4G**). Moreover, these 4 clusters also showed increased expression of GC-associated markers (Fas or PNA), compared to other clusters (**Figure 4G**). On the other hand, the clusters that had a higher frequency in the control mice compared to the cKO (cluster 6, 9, and 8) showed increased PR8-HA staining and IRF4 expression (**Figure 4G**) indicating increase in plasma cells recognizing infecting virus. Thus, loss of αv promotes sustained increase in GC B cells of IgA isotype with increased cross-reactivity.

It was difficult to perform a similar cluster analysis on memory B cells as our memory B cell gating was based on identification cells that are not naïve, GC or plasma cells. To perform a similar cluster analysis on memory B cells we decided to re-challenge the mice as we predicted this would lead to expansion of antigen-specific memory B cells and provide positive markers for memory B cells, such as CD73. We analyzed memory B cells at day 4 post re-challenge, when the memory response should be at peak. We performed PhenoGraph cluster analysis within the lung-resident IgD^- memory B cells and identified clusters showing increased frequency of cells in the cKO mice, which were cluster 8, 1, 6 and 7. These 4 clusters were highly positive for Cal09-HA and the marker CD73 **(Figure 4H)**. There was only one cluster showing high IgA expression, cluster 8. This was one of the clusters with increased frequency of cells in the cKO mice and showed high CD73 expression as well as increased staining for Cal09-HA. CD73 is a marker associated with GC derived memory B cells[22], therefore these findings indicate that the loss of B cell αv leads to sustained increase in GC B cells in the lungs after influenza infection, which leads to increases in cross-reactive IgA memory B cells.

To confirm that the sustained increase in lung-resident IgA+ GC B cells and IgA memory B cells in the cKO mice, is due to ongoing GC reactions in the lungs, we also investigated the persistence of iBALT structures. At day 36 post infection, we continued to see increases in IgA+ cells in the lungs from cKO mice (**Figure 5A**). At this time point, iBALT-GC areas in the lungs of control mice had a similar size to the cKO, agreeing with the kinetics of later development of GC structures in the lungs from control mice (**Figure 5A-B**). However, GL7 staining intensity within these areas was clearly higher in the lungs from cKO mice (**Figure 5A and C**), indicating continued accumulation of GC clusters in the lungs of cKO mice. We observed minimal IgA+ cells in the GC areas in the control lungs (**Figure 5A**) and quantification confirmed that both the area of IgA+ cells (**Figure 5D**) and the percentage of IgA+ and GL7+ cells (**Figure 5E**) within the iBALT-GC structures continued to be higher in the cKO lungs compared to the control. Additionally, confirming our flow cytometry data, we also observed Cal09-HA+ cells within the GC areas in the cKO lungs, but these were not seen in the control lungs (**Figure 5F-G**). Together, these data establish that αv deletion from B cells leads to prolonged germinal center reactions in the lung upon intranasal infection with influenza virus, and this increase in germinal center reactions promotes increase in IgA memory B cells cross-reactive to antigenic variants of the antigens from the infecting virus.

B cell αv integrin regulates IgA class-switch recombination in a B cell intrinsic manner

Our previous studies showed that αv integrins have a B cell intrinsic role in limiting TLR signaling, and this regulates the ability of B cells to differentiate in response to TLR ligands and TLR ligand containing antigens. To confirm whether this increase in differentiation of IgA isotype B cells in the lungs of cKO mice is also related to this B cell intrinsic role of αv, we used *in vitro* cultures for differentiation of B cells with TLR ligand stimulation. To specifically investigate B cell isotype switching related to influenza infection, we used TLR7 ligand stimulation. Total B cells isolated from either lung (i.v. $CD45^-$ lung-resident) or spleen were stimulated with TLR7 ligand R848 and the IgA+ cells generated in culture were analyzed by flow cytometry. This analysis showed that R848 stimulation alone was sufficient to drive differentiation of lung B cells into IgA isotype B cells in culture. Differentiation to IgA B cells was increased in the cultures with lung B cells from cKO mice compared to cultures from lung B cells from control mice (**Figure 6A**), indicating that enhanced TLR signaling due to loss of B cell αv promotes increases in IgA B cell differentiation. The percentages of IgA+ cells generated in these cultures were low and we also found that cultures from spleen B cells with R848 alone, did not significantly induce IgA differentiation (**Figure 6B**) therefore we turned to more elaborate cultures to assess in more detail the role of αv integrins in regulating IgA B cell differentiation.

We adapted an *in vitro* culture system previously described[23, 24] to generate sufficient antibody-secreting cells (ASCs) that have class-switched to IgA. To ascertain whether the effect of αv on IgA class switching was specific to tissue residency, we isolated total B cells from either lung (i.v. $CD45^-$ lung-resident), spleen or medLN. We verified that the starting cells were not IgA+ and initiated the culture system by subjecting these B cells to signals they would likely encounter during activation *in vivo*. To further establish whether the regulation of TLR signaling by the αv integrin on B cells is involved in IgA B cell differentiation, we chose TLR9 ligand CpG for the initial activation signal. Following this two-day activation period we next simulated the cells with signals that B cells would encounter in their interactions with T cells during germinal center-like reactions. The B cells were plated over feeder cells that secreted the B cell survival cytokine B cell activating factor (BAFF) and expressed the T cell costimulatory molecule CD40L. To this culture we added IL-21 and signals known to control IgA class-switch recombination, retinoic acid and

TGFβ. Following three days in this Phase I culture, we transitioned the B cells into a three-day Phase II culture over the feeder cells in the presence of IL-21 alone to drive the differentiation of ASCs. Following this eight-day culture system we assessed the phenotype of the B cells by flow cytometry (**Figure 6C**).

Flow cytometry showed that cultures from both control and cKO lungs led to generation of IgA+ cells induced by culture conditions. However, cultures of cKO B cells, from the lungs led to significant increase in percentage of IgA isotype plasma cells (IRF4+ cells), compared to cultures from control B cell cultures (**Figure 6D**). ELISA on culture supernatants further confirmed an increase in IgA antibody secretion in the cKO lung B cell cultures, compared to the control cultures (**Figure 6E**). Additionally, we found that cultures of B cells from medLNs also led to development of IgA isotype plasma cells, but the increase in IgA+ cells in the cKO compared to control cultures was smaller (**Figure 6F**). The spleen cultures from cKO mice showed a better increase in IgA+ cells compared to the medLNs although the fold increase in this case was still less than what was seen in the lung B cell cultures (**Figure 6F-G**).

Thus, these data indicate that enhanced TLR signaling due to loss of B cell αv promotes increases in IgA B cell differentiation. While the effect of αv regulation of IgA B cell differentiation is most pronounced in the B cells from the lung microenvironment, given appropriate stimulation this can also be observed in B cells from other tissues such as the spleen and medLN.

Discussion

Recent studies have shown that natural infection of the respiratory tract by influenza virus induces memory B cells that are lung resident[1], major producers of broadly-reactive antibodies[15] and the protective antibodies of the IgA isotype[1, 2]. These lung-resident cells are known to contribute significantly to increased protection from secondary infection, but they are not generated by systemic immunization strategies. Despite these important findings, we still do not know the mechanisms regulating lung B cell responses, specifically it is not clear how the lung IgA B cell responses arise and how they are maintained. Understanding the signals that regulate the generation of these lung-resident B cell populations will be critical to developing better intranasal immunization strategies to combat influenza and other mucosal respiratory viruses. Our data indicate that αv integrin restricts development of lung-resident IgA memory B cells, through its B cell intrinsic role on regulation of TLR signaling. Therefore, deletion of αv integrins from B cells promotes beneficial B cell responses in the lungs during viral infection. Loss of B cell αv promotes a sustained increase in GC reactions occurring locally in the lungs (**Figures 3 and 5**), which drive increases in cross-reactive lung-resident IgA memory B cells (**Figure 4**), after infection with influenza virus. These data show that IgA+ B cells in the lungs can be generated and maintained through GC reactions occurring in the lungs and manipulating αv integrins could provide a way to promote durable IgA memory B cell responses in the lungs against respiratory viruses. Although we have previously shown a role for αv in promoting GC reactions after systemic immunization, the significance of these findings is that the loss of B cell αv promotes GC reactions in tissue sites, such as lungs, where it is difficult to induce such responses.

GCs are sites of affinity maturation of B cells, where B cells undergo successive rounds of proliferation, SHM and selection, through antigen presentation to T follicular helper (Tfh) cells[25]. Studies on influenza and other viral infections have revealed increasing SHM in the GCs not only increases the affinity of B cells and resulting antibodies to the immunizing antigen, but continued SHM also increase the breadth of responses to viral proteins, allowing generation of antibodies able to target multiple strains[26, 27]. We have

previously shown that the absence of B cell αv integrins leads to increase in antigen- and TLR signal-induced GC reactions. As a result, B cells from mice lacking B cell αv, show increases in SHM in the IgG antibody heavy chain after systemic vaccination with virus-like particles[14]. These studies also showed that after immunization with H1N1 PR8 strain, mice lacking αv on B cells exhibit increased antibody response to HA from the PR8 strain, as well as to the heterologous Cal09 strain, indicating higher levels of mutations in the αv-deficient B cells allowed them to expand the diversity of epitopes recognized. Thus, the increase in lung-resident GCs, memory B cells and plasma cells recognizing Cal09-HA in the cKO mice, following PR8 IAV intranasal infection, correlates with our previous findings and we predict this is related to the increased GC reactions occurring locally in the lungs. While we have not investigated cross-reactivity to further divergent influenza strains, based on the increase in GC reactions, we predict we would see an increase in the breadth of reactivity of antibodies produced in the lungs of cKO mice towards multiple antigenic variants of influenza virus. Moreover, previous studies have indicated that lung GC reactions lead to memory B cells with greater cross protective potential compared to B cells from spleen[15] and our studies show that blockade of αv on B cells could be used to promote this feature.

Apart from SHM and affinity maturation of antibodies, GC reactions are key also for the development of long-lived memory B cells and plasma cells, critical for protective immunity against multiple pathogens[28]. However, these GC reactions are a prominent feature of secondary lymphoid organs. While GC structures had been described in the lungs after infection, the importance of these tissue-resident GC structures for protective immunity and sustained memory response is still being established. Previous studies have shown that upon influenza infection, structures with similar compartmentalization and cellular composition to secondary lymphoid organs, termed iBALT, are ectopically generated in the lungs of mice and support GC B cell proliferation[17, 29], even in the absence of secondary lymphoid organs[30]. Although the presence of iBALT in healthy adult humans has been controversial [31], a recent study has shown that these iBALT associated GC structures are present in lungs from children and are involved in the immune response to respiratory viruses[16]. A previous study has also shown that type I interferon induced CXCL13 production by lung fibroblast populations is important in driving the establishment of these iBALT-GC reactions[18]. However, it is still not known whether these lung GC structures support the generation of IgA isotype B cells, and whether IgA memory B cells in the lungs are derived from GC reactions in the lungs. Our studies establish that IgA B cells in the lungs can arise from GC reactions occurring in the lungs (**Figures 3 and 5**) and that B cell intrinsic αv signal is important in regulating this process.

We have previously shown that the loss of B cell αv enhances responses from innate B cell populations such as B1 B cells, Marginal zone B cells, as well as extrafollicular B cells[4, 13]. These B cell populations can all be involved in the immune response against respiratory viruses[32] and likely lead to early IgA production at the respiratory tract. However, our data show a clear connection between IgA+ B cells and GC reactions in the lungs, related to more sustained IgA production in the absence of B cell αv. Our flow cytometry analysis showed an increase in IgA+ B cells that are cross-reactive to Cal09-HA and show markers of GC cells in the cKO mice at 35 days after infection (**Figure 4**). Similarly, our microscopy data also showed a clear increase in GC structures and IgA+ B cells within these structures in the lungs of cKO mice, compared to the lungs from control mice (**Figures 3 and 5**). These data, together with the flow cytometry data showing that majority of IgA+ B cells are found in the lungs and are non-recirculating (**Figure 2** and **Sup Figure 4**), indicate that IgA+ GC and memory B cells are generated in the iBALT areas in the lungs, and deletion of B cell αv integrin promotes these B cells by sustaining GC reactions in the lungs. After re-infection we find an increase in CD73+ IgA+ and Cal09-HA+ memory B cells in the lungs of cKO mice

compared to the lungs of control mice (**Figure 4**). CD73+ memory B cells are thought to be GC-derived, and while we cannot rule out the possibility that these memory B cells could be generated from GC reactions in the medLN, based on our data demonstrating relative lack of IgA+ B cells in the medLNs (**Sup Figure 4**), we predict that the increase in cross-reactive IgA memory B cells in the lungs of cKO mice are at least in part due to increased GC reactions in the lungs.

It is likely that influenza infection is also leading to increases in the IgG isotype B cells in the medLN and spleen in the cKO mice, which could contribute towards protective immunity. We have specifically focused on the IgA isotype B cells in this study because the relevance of GC reactions in the development of IgA isotype B cells in respiratory sites, such as the lungs, is still not clear. TGFβ dependent mechanisms are known to be important for the generation of IgA B cells in subsets of germinal center B cells in the intestinal mucosa[33], but the mechanisms regulating IgA class switching in the lungs have not been explored. Similarly, the role of TLR signaling in class switching in the lungs is also not clear. While TLR signaling may not be a requirement for generation of IgA B cells, our data suggest that enhancing TLR signaling is enough to increase class switching to IgA isotype B cells, and this is particularly relevant for the B cells from the lung microenvironment. This could be related to specific aspects of B cells that have interacted with TLR ligand signals in lung mucosa. In previous studies, we have shown that loss of αv from B cells leads to increase in *Aicda* gene expression, related to TLR signaling[12, 14]. This increased expression could explain increases in both class-switching and SHM observed in the αv cKO B cells. It is also possible that increases in TLR signaling in the αv-deficient B cells allow for better antigen presentation and generation of memory B cells, as these cells require antigen encounter in the lungs[1]. Our data suggest that the lung microenvironment is equipped with special regulatory mechanism to limit IgA class switching, and this mechanism could be also promoted in other tissues such as the spleen through enhancing TLR signaling. These lung specific regulatory mechanisms could be utilized to specifically promote immune responses against respiratory pathogens. Moreover, our studies indicate that αv blockade could also be used to promote IgA responses through systemic immune response.

The increase in lung GC reactions in the cKO mice leads to questions about their functional capacity for protection. The marked increase in CD73+ IgA memory B cells in the cKO mice, suggests that these GC reactions result in an expanded memory response and thus likely confers better protection. Nonetheless, we were not able to address the contribution of IgA memory B cells in leading to protection after challenge studies, as we observed higher numbers of both IgG and IgA secreting cells in the lungs of cKO mice. Future studies are required to address the protective capacity of IgG versus IgA antibodies in driving protection and are beyond the scope of this study. However, our previous studies have demonstrated that the B cell specific αv knockout mice show better protection after a lethal intranasal infection, indicating the protective capacity of the lung-resident B cell responses in these mice[14]. Moreover, it has been proposed that HA-specific IgA, rather than IgG responses generated in the lung, are responsible for cross-strain protection from different IAV subtypes[34], indicating the key role of IgA antibodies in protection from respiratory mucosal viruses. Thus, we predict that the increased GC derived IgA responses in the cKO mice plays a major role in conferring superior protection compared to the IgG B cells in the event of a mucosal challenge. In further studies, we are exploring intranasal immunization strategies that would induce a similar expanded GC reaction in the cKO mice, which would allow us to harness the beneficial features of loss of B cell αv for vaccine studies.

Memory B cells capable of neutralizing multiple strains of the same pathogen have been identified in humans after influenza or HIV infection, but efforts to develop vaccines that induced broadly protective memory B cell response to pathogens have not yet been successful. Similarly, multiple recent studies have shown the advantages of IgA inducing intranasal vaccines for blocking infection and transmission of respiratory viruses compared to systemic vaccines[2, 35, 36]. But it has proven challenging to develop intranasal vaccines that lead to long-lived protection at the respiratory tract. Strategies that can promote GC reactions in the lungs could be beneficial to drive both broadly reactive and long-lived IgA memory B cells that are lung-resident. In this context, blockade of B cell αv could be used to improve efficacy of intranasal respiratory virus vaccines, as they could enhance multiple aspects of protective immune response against respiratory viruses, including, tissue-resident GC reactions, IgA isotype B cells, breadth of reactivity of B cells to evolving strains, and lung-resident memory B cell responses. Drugs and antibodies targeting the αv family of integrins have been tested therapeutically in other disease settings such as cancer, and therefore could be utilized for αv-blockade on immune cells. Thus, these studies using the B cell specific αv-deficient mouse model have allowed us to understand unique mechanisms in the lung microenvironment that control lung-resident IgA memory B cell responses and identified new strategies to promote immune responses directly at the respiratory tract for more effective respiratory virus vaccines.

Materials and Methods

Mice

$\alpha v^{fl/fl}$ mice were backcrossed to C57BL/6J mice as previously described[11, 14]. The animals were bred and maintained on the C57BL/6 background. $\alpha v^{fl/fl}$ mice were crossed with CD19 cre transgenic mice to generate B cell specific αv knockout mice, referred to as conditional KO (cKO) mice ($CD19^{cre/+}$ $\alpha v^{fl/fl}$). Mice with a single $CD19^{Cre}$ allele, $CD19^{cre/+}\alpha v^{+/+}$ were used as controls. For *in vitro* experiments C57BL/6 mice were used as controls. All mice for this study were age and sex-matched and were 9-14 weeks old at the time of infection or vaccination. Mice were housed in a specific pathogen-free facility. All procedures were approved by the Institutional Animal Care and Use Committee at Seattle Children's Research Institute.

Influenza infection

Live PR8 IAV was purchased from Charles River Laboratories and stored in one-use aliquots at -80°C. Just prior to infection, PR8 was thawed and diluted in PBS. Mice were anesthetized with Isoflurane (Patterson Veterinary) and infected with PR8 IAV in 25µL in the nostrils. Mice were weighed and monitored for signs and symptoms of disease for the duration of the study.

HA tetramer preparation

The B cell HA tetramers were either a gift from Dr. Emily Gage[37] or from Dr. Kanekiyo Masaru's lab at NIH. Tetramers with an AviTag were biotinylated with the BirA biotin-ligase kit (Avidity) according to manufacturer's instructions. Following biotinylation, BV711- (BioLegend) or PerCpCy5.5- (BioLegend) conjugated streptavidin was added in 5 serial steps with a 10-minute incubation period each to the unlabeled tetramers. Labeled tetramers were prepared the day before the experiment.

Antibodies

α-IgD-BV786, α-B220-BUV395, α-CD45-BUV395, α-CD19-BUV737 were purchased from BD Horizon. A-CD3-BV510, α-CD11c-BV510, α-F4/80-BV510, α-CD138-BV421, α-Fas-BV605, Streptavidin (SA)-PerCPCy5.5, SA-BV711 and α-IgM-PerCPCy5.5 were from BioLegend. α-CD45-APC, α-IRF4-PeCy7 and α-IRF4-AF700 were purchased from Invitrogen. α-IgA-Biotin, α-IgA-PE and α-IgM-PeCy7 were from Southern Biotech. α-Gr1-BV510 and PNA-FITC were from Miltenyi Biotechnologies and Vector Labs, respectively.

Flow cytometry

5 minutes prior to euthanasia, mice were injected with 1μg α-CD45-BUV395 or α-CD45-APC in the retro-orbital cavity. Lungs and mediastinal lymph nodes (medLN) were collected from euthanized mice. Lung tissue was digested with 1.5mg/mL collagenase (Milipore Sigma) and 10μg/mL DNAse I (Milipore Sigma) in Mg^{2+}, Ca^{2+} free Hank's balanced salt solution (HBSS, Gibco) with 10% fetal bovine serum (FBS, Sigma) for 1 hr at 37°C or 30 min in a shaking incubator at 1000 rpm. Lungs and medLN were then ground into a 40μm filter to generate a single cell suspension. For some experiments lung B cells were isolated using CD19 positive magnetic bead separation (STEMCell). Cells were counted using AccuCheck count beads (ThermoFisher) or Muse Cell Analyzer (Luminex) according to the manufacturer's instructions. Cells were then stained with fixable LiveDead Aqua (ThermoFisher) to identify dead cells, after which cells were stained with PR8-HA and Cal09-HA B cell tetramers and surface antibodies for 20 minutes at room temperature. To identify intracellular antigens, cells were then fixed and permeabilized with the Transcription Factor kit (BioLegend) according to manufacturer's instructions. Events were analyzed on an LSRII flow cytometer (BD Biosciences) or an LSR Fortessa (BD Biosciences) and analyzed using FlowJo (v.10, TreeStar). See Supplemental **Figure 1** for gating strategies.

ELISpot

ELISpots were performed on single cell suspensions of lung or medLN cells, prepared as described above. MAIPS ELISpot plates (Millipore) were pre-coated with 3μg/mL PR8-HA or Cal09-HA (SinoBiological) diluted in PBS. Serial dilutions of cells were plated over wells and incubated over night at 37°C. Spots were developed using α-mouse IgG or α-mouse IgA alkaline phosphatase (AP) Abs (Southern Biotech) followed by BCIP/NBT AP substrate (Vectors Labs). Spots were imaged and counted using an ImmunoSpot analyzer (Cellular Technology Limited).

Histology and Immunofluorescence

Lungs were perfused with PBS and then inflated and embedded in OCT, and frozen at -80C (as described in[38]). Frozen sections (8μm) were fixed in acetone at -20C, air dried and blocked with 1% normal goat serum (Jacskon ImmunoResearch) and 1% BSA (Sigma) in PBS with 0.1% Tween-20 (Sigma). Slides were stained with Hoescht, α-CD19-AF647, α-GL7-FITC and α-IgA-PE. Images were acquired with a Zeiss LSM 900 confocal microscope. Image processing and analysis were performed with FIJI (ImageJ) software[39], with a personalized macro where the iBALT structure was manually delimited by the polygon tool, and then the image was converted to a mask by default threshold to measure the area of IgA and GL7 positive staining by the "analyze particle" function. IgA+GL7+ positive area percentage was calculated by applying the image Calculator "AND" function over IgA and GL7 masks, then measuring the resulting area by analyze particle function and calculating the percentage of the resulting area over the whole GL7 positive area.

In vitro plasma cell culture

All mice were injected retro orbitally with 1µg αCD45-BUV395 5 minutes prior to euthanasia. B cells from spleen, medLN or lung were isolated using negative magnetic bead separation (STEMCell). Cultures with R848 only were performed on lympholyte-M (Cedarlane) separated lung B cells and B cells from spleen isolated using negative magnetic bead separation. $B220^+$ B cells were then sorted for i.v. $CD45^-$ populations using an Aria FACS sorter (BD Biosciences). Plasma cells were differentiated from naive B cells. Briefly, cells were suspended in Iscove's modified Dulbecco's medium (IMDM, cytiva) supplemented with 10% FBS (Sigma), 2mM Glutamax (Gibco), 55µM β-mercaptoethanol (Gibco), 100U/mL penicillin (Gibco) and 100µg/mL streptomycin (Gibco) and activated with 1µg/mL CpG (Invivogen) for two days. Cells were then seeded over irradiated 40LB feeder cells, a generous gift from Dr. Daisuke Kitamura[24], expressing mouse CD40L and BAFF. To induce class switch to IgA, cells were incubated with 2ng/mL TGF-β (BioLegend), 100nM retinoic acid (RA, Sigma) and 40ng/mL IL-21 (Peprotech) for three days, followed by three days in IL-21 alone.

ELISA

Enzyme linked immunosorbent assays (ELISAs) were performed on the supernatant of cultured cells (see *in vitro* plasma cell culture for culture details). Immulon 2HB plates (ThermoFisher) were pre-coated with 2µg/mL of goat-α-mouse Ig(H+L) (Southern Biotech) diluted in PBS. Serial dilutions of supernatant were plated and left overnight at 4°C. The plates were developed using α-mouse IgA-AP Abs (Southern Biotech) followed by 4-Nitropenyl phosphate disodium salt hexahydrate substrate tablets (Sigma). Absorbance was measured using a Spectramax 190 luminometer (Molecular Devices) at 405 nm.

Statistical analysis

Raw data from control and cKO PR8-infected groups were analyzed by Mann-Whiney U test or 2-way ANOVA using GraphPad Prism (v.9.3.1). $p<0.05$ were considered statistically significant.

Acknowledgements

We thank Sara Sagadiev, Aaron Liu and Ursula Holder for laboratory assistance and useful insights and discussion. This research was supported by the Office of Animal Care, the Microscopy and Histopathology CoLab and the Flow Cytometry Core at Seattle Children's Research Institute.

Funding

This work was supported by National Institute of Health R01 AI151167 (to M.A.)

References

1. Allie SR, Bradley JE, Mudunuru U, Schultz MD, Graf BA, Lund FE, Randall TD. The establishment of resident memory B cells in the lung requires local antigen encounter. Nat Immunol. 2019;20(1):97-108. Epub 2018/12/05. doi: 10.1038/s41590-018-0260-6. PubMed PMID: 30510223; PMCID: PMC6392030.
2. Oh JE, Song E, Moriyama M, Wong P, Zhang S, Jiang R, Strohmeier S, Kleinstein SH, Krammer F, Iwasaki A. Intranasal priming induces local lung-resident B cell populations that secrete protective mucosal antiviral IgA. Sci Immunol. 2021;6(66):eabj5129. Epub 20211210. doi: 10.1126/sciimmunol.abj5129. PubMed PMID: 34890255; PMCID: PMC8762609.

3. Acharya M, Edkins AL, Ozanne BW, Cushley W. SDF-1 and PDGF enhance alphavbeta5-mediated ERK activation and adhesion-independent growth of human pre-B cell lines. Leukemia. 2009;23(10):1807-17. doi: 10.1038/leu.2009.126. PubMed PMID: 19609283.
4. Acharya M, Mukhopadhyay S, Paidassi H, Jamil T, Chow C, Kissler S, Stuart LM, Hynes RO, Lacy-Hulbert A. alphav Integrin expression by DCs is required for Th17 cell differentiation and development of experimental autoimmune encephalomyelitis in mice. J Clin Invest. 2010;120(12):4445-52. doi: 10.1172/JCI43796. PubMed PMID: 21099114; PMCID: PMC2993596.
5. Gianni T, Leoni V, Chesnokova LS, Hutt-Fletcher LM, Campadelli-Fiume G. alphavbeta3-integrin is a major sensor and activator of innate immunity to herpes simplex virus-1. Proc Natl Acad Sci U S A. 2012;109(48):19792-7. doi: 10.1073/pnas.1212597109. PubMed PMID: 23150579; PMCID: PMC3511702.
6. Lacy-Hulbert A, Smith AM, Tissire H, Barry M, Crowley D, Bronson RT, Roes JT, Savill JS, Hynes RO. Ulcerative colitis and autoimmunity induced by loss of myeloid alphav integrins. Proc Natl Acad Sci U S A. 2007;104(40):15823-8. Epub 2007/09/27. doi: 10.1073/pnas.0707421104. PubMed PMID: 17895374; PMCID: PMC1994135.
7. Lucas M, Stuart LM, Savill J, Lacy-Hulbert A. Apoptotic cells and innate immune stimuli combine to regulate macrophage cytokine secretion. J Immunol. 2003;171(5):2610-5. Epub 2003/08/21. doi: 10.4049/jimmunol.171.5.2610. PubMed PMID: 12928413.
8. Overstreet MG, Gaylo A, Angermann BR, Hughson A, Hyun YM, Lambert K, Acharya M, Billroth-Maclurg AC, Rosenberg AF, Topham DJ, Yagita H, Kim M, Lacy-Hulbert A, Meier-Schellersheim M, Fowell DJ. Inflammation-induced interstitial migration of effector CD4(+) T cells is dependent on integrin alphaV. Nat Immunol. 2013;14(9):949-58. doi: 10.1038/ni.2682. PubMed PMID: 23933892; PMCID: PMC4159184.
9. Savill J, Dransfield I, Hogg N, Haslett C. Vitronectin receptor-mediated phagocytosis of cells undergoing apoptosis. Nature. 1990;343(6254):170-3. doi: 10.1038/343170a0. PubMed PMID: 1688647.
10. Schrock DC, Leddon SA, Hughson A, Miller J, Lacy-Hulbert A, Fowell DJ. Pivotal role for alphaV integrins in sustained Tfh support of the germinal center response for long-lived plasma cell generation. Proc Natl Acad Sci U S A. 2019. doi: 10.1073/pnas.1809329116. PubMed PMID: 30770452; PMCID: PMC6410787.
11. Acharya M, Sokolovska A, Tam JM, Conway KL, Stefani C, Raso F, Mukhopadhyay S, Feliu M, Paul E, Savill J, Hynes RO, Xavier RJ, Vyas JM, Stuart LM, Lacy-Hulbert A. alphav Integrins combine with LC3 and atg5 to regulate Toll-like receptor signalling in B cells. Nat Commun. 2016;7:10917. doi: 10.1038/ncomms10917. PubMed PMID: 26965188; PMCID: PMC4792966.
12. Muir V, Sagadiev S, Liu S, Holder U, Armendariz AM, Suchland E, Meitlis I, Camp N, Giltiay N, Tam JM, Garner EC, Wivagg CN, Shows D, James RG, Lacy-Hulbert A, Acharya M. Transcriptomic analysis of pathways associated with ITGAV/alpha(v) integrin-dependent autophagy in human B cells. Autophagy. 2023;19(3):926-42. Epub 20220825. doi: 10.1080/15548627.2022.2113296. PubMed PMID: 36016494.
13. Acharya M, Raso F, Sagadiev S, Gilbertson E, Kadavy L, Li QZ, Yan M, Stuart LM, Hamerman JA, Lacy-Hulbert A. B Cell alphav Integrins Regulate TLR-Driven Autoimmunity. J Immunol. 2020;205(7):1810-8. Epub 2020/08/30. doi: 10.4049/jimmunol.1901056. PubMed PMID: 32859730; PMCID: PMC7504890.
14. Raso F, Sagadiev S, Du S, Gage E, Arkatkar T, Metzler G, Stuart LM, Orr MT, Rawlings DJ, Jackson SW, Lacy-Hulbert A, Acharya M. alphav Integrins regulate germinal center B cell responses through noncanonical autophagy. J Clin Invest. 2018;128(9):4163-78. Epub 2018/07/13. doi: 10.1172/JCI99597. PubMed PMID: 29999501; PMCID: PMC6118577.

15. Adachi Y, Onodera T, Yamada Y, Daio R, Tsuiji M, Inoue T, Kobayashi K, Kurosaki T, Ato M, Takahashi Y. Distinct germinal center selection at local sites shapes memory B cell response to viral escape. J Exp Med. 2015;212(10):1709-23. doi: 10.1084/jem.20142284. PubMed PMID: 26324444; PMCID: PMC4577849.
16. Matsumoto R, Gray J, Rybkina K, Oppenheimer H, Levy L, Friedman LM, Khamaisi M, Meng W, Rosenfeld AM, Guyer RS, Bradley MC, Chen D, Atkinson MA, Brusko TM, Brusko M, Connors TJ, Luning Prak ET, Hershberg U, Sims PA, Hertz T, Farber DL. Induction of bronchus-associated lymphoid tissue is an early life adaptation for promoting human B cell immunity. Nat Immunol. 2023;24(8):1370-81. Epub 20230717. doi: 10.1038/s41590-023-01557-3. PubMed PMID: 37460638; PMCID: PMC10529876.
17. Moyron-Quiroz JE, Rangel-Moreno J, Kusser K, Hartson L, Sprague F, Goodrich S, Woodland DL, Lund FE, Randall TD. Role of inducible bronchus associated lymphoid tissue (iBALT) in respiratory immunity. Nat Med. 2004;10(9):927-34. Epub 20040815. doi: 10.1038/nm1091. PubMed PMID: 15311275.
18. Denton AE, Innocentin S, Carr EJ, Bradford BM, Lafouresse F, Mabbott NA, Morbe U, Ludewig B, Groom JR, Good-Jacobson KL, Linterman MA. Type I interferon induces CXCL13 to support ectopic germinal center formation. J Exp Med. 2019;216(3):621-37. Epub 20190205. doi: 10.1084/jem.20181216. PubMed PMID: 30723095; PMCID: PMC6400543.
19. de Carvalho RVH, Ersching J, Barbulescu A, Hobbs A, Castro TBR, Mesin L, Jacobsen JT, Phillips BK, Hoffmann HH, Parsa R, Canesso MCC, Nowosad CR, Feng A, Leist SR, Baric RS, Yang E, Utz PJ, Victora GD. Clonal replacement sustains long-lived germinal centers primed by respiratory viruses. Cell. 2023;186(1):131-46 e13. Epub 20221223. doi: 10.1016/j.cell.2022.11.031. PubMed PMID: 36565697; PMCID: PMC9870066.
20. Kanekiyo M, Joyce MG, Gillespie RA, Gallagher JR, Andrews SF, Yassine HM, Wheatley AK, Fisher BE, Ambrozak DR, Creanga A, Leung K, Yang ES, Boyoglu-Barnum S, Georgiev IS, Tsybovsky Y, Prabhakaran MS, Andersen H, Kong WP, Baxa U, Zephir KL, Ledgerwood JE, Koup RA, Kwong PD, Harris AK, McDermott AB, Mascola JR, Graham BS. Mosaic nanoparticle display of diverse influenza virus hemagglutinins elicits broad B cell responses. Nat Immunol. 2019;20(3):362-72. Epub 20190211. doi: 10.1038/s41590-018-0305-x. PubMed PMID: 30742080; PMCID: PMC6380945.
21. Chen H, Lau MC, Wong MT, Newell EW, Poidinger M, Chen J. Cytofkit: A Bioconductor Package for an Integrated Mass Cytometry Data Analysis Pipeline. PLoS Comput Biol. 2016;12(9):e1005112. Epub 20160923. doi: 10.1371/journal.pcbi.1005112. PubMed PMID: 27662185; PMCID: PMC5035035.
22. Conter LJ, Song E, Shlomchik MJ, Tomayko MM. CD73 expression is dynamically regulated in the germinal center and bone marrow plasma cells are diminished in its absence. PLoS One. 2014;9(3):e92009. Epub 20140324. doi: 10.1371/journal.pone.0092009. PubMed PMID: 24664100; PMCID: PMC3963874.
23. Hung KL, Meitlis I, Hale M, Chen CY, Singh S, Jackson SW, Miao CH, Khan IF, Rawlings DJ, James RG. Engineering Protein-Secreting Plasma Cells by Homology-Directed Repair in Primary Human B Cells. Mol Ther. 2018;26(2):456-67. Epub 2017/12/24. doi: 10.1016/j.ymthe.2017.11.012. PubMed PMID: 29273498; PMCID: PMC5835153.
24. Nojima T, Haniuda K, Moutai T, Matsudaira M, Mizokawa S, Shiratori I, Azuma T, Kitamura D. In-vitro derived germinal centre B cells differentially generate memory B or plasma cells in vivo. Nat Commun. 2011;2:465. Epub 20110906. doi: 10.1038/ncomms1475. PubMed PMID: 21897376.
25. Victora GD, Nussenzweig MC. Germinal centers. Annu Rev Immunol. 2012;30:429-57. doi: 10.1146/annurev-immunol-020711-075032. PubMed PMID: 22224772.
26. Corti D, Bianchi S, Vanzetta F, Minola A, Perez L, Agatic G, Guarino B, Silacci C, Marcandalli J, Marsland BJ, Piralla A, Percivalle E, Sallusto F, Baldanti F, Lanzavecchia A. Cross-neutralization of four paramyxoviruses by a human monoclonal antibody. Nature. 2013;501(7467):439-43. doi: 10.1038/nature12442. PubMed PMID: 23955151.

27. Pappas L, Foglierini M, Piccoli L, Kallewaard NL, Turrini F, Silacci C, Fernandez-Rodriguez B, Agatic G, Giacchetto-Sasselli I, Pellicciotta G, Sallusto F, Zhu Q, Vicenzi E, Corti D, Lanzavecchia A. Rapid development of broadly influenza neutralizing antibodies through redundant mutations. Nature. 2014;516(7531):418-22. doi: 10.1038/nature13764. PubMed PMID: 25296253.
28. Matz HC, McIntire KM, Ellebedy AH. 'Persistent germinal center responses: slow-growing trees bear the best fruits'. Curr Opin Immunol. 2023;83:102332. Epub 20230505. doi: 10.1016/j.coi.2023.102332. PubMed PMID: 37150126; PMCID: PMC10829534.
29. Tan HX, Esterbauer R, Vanderven HA, Juno JA, Kent SJ, Wheatley AK. Inducible Bronchus-Associated Lymphoid Tissues (iBALT) Serve as Sites of B Cell Selection and Maturation Following Influenza Infection in Mice. Front Immunol. 2019;10:611. Epub 20190329. doi: 10.3389/fimmu.2019.00611. PubMed PMID: 30984186; PMCID: PMC6450362.
30. Moyron-Quiroz JE, Rangel-Moreno J, Hartson L, Kusser K, Tighe MP, Klonowski KD, Lefrancois L, Cauley LS, Harmsen AG, Lund FE, Randall TD. Persistence and responsiveness of immunologic memory in the absence of secondary lymphoid organs. Immunity. 2006;25(4):643-54. doi: 10.1016/j.immuni.2006.08.022. PubMed PMID: 17045819.
31. Tschernig T, Pabst R. Bronchus-Associated Lymphoid Tissue (BALT) Is Not Present in the Normal Adult Lung but in Different Diseases. Pathobiology. 2000:1-8.
32. Baumgarth N. How specific is too specific? B-cell responses to viral infections reveal the importance of breadth over depth. Immunol Rev. 2013;255(1):82-94. Epub 2013/08/21. doi: 10.1111/imr.12094. PubMed PMID: 23947349; PMCID: PMC3748619.
33. Reboldi A, Arnon TI, Rodda LB, Atakilit A, Sheppard D, Cyster JG. IgA production requires B cell interaction with subepithelial dendritic cells in Peyer's patches. Science. 2016;352(6287):aaf4822. doi: 10.1126/science.aaf4822. PubMed PMID: 27174992; PMCID: PMC4890166.
34. Okuya K, Yoshida R, Manzoor R, Saito S, Suzuki T, Sasaki M, Saito T, Kida Y, Mori-Kajihara A, Kondoh T, Sato M, Kajihara M, Miyamoto H, Ichii O, Higashi H, Takada A. Potential Role of Nonneutralizing IgA Antibodies in Cross-Protective Immunity against Influenza A Viruses of Multiple Hemagglutinin Subtypes. J Virol. 2020;94(12). Epub 20200601. doi: 10.1128/JVI.00408-20. PubMed PMID: 32269119; PMCID: PMC7307104.
35. Hassan AO, Kafai NM, Dmitriev IP, Fox JM, Smith BK, Harvey IB, Chen RE, Winkler ES, Wessel AW, Case JB, Kashentseva E, McCune BT, Bailey AL, Zhao H, VanBlargan LA, Dai YN, Ma M, Adams LJ, Shrihari S, Danis JE, Gralinski LE, Hou YJ, Schafer A, Kim AS, Keeler SP, Weiskopf D, Baric RS, Holtzman MJ, Fremont DH, Curiel DT, Diamond MS. A Single-Dose Intranasal ChAd Vaccine Protects Upper and Lower Respiratory Tracts against SARS-CoV-2. Cell. 2020;183(1):169-84 e13. Epub 20200819. doi: 10.1016/j.cell.2020.08.026. PubMed PMID: 32931734; PMCID: PMC7437481.
36. Hassan AO, Shrihari S, Gorman MJ, Ying B, Yuan D, Raju S, Chen RE, Dmitriev IP, Kashentseva E, Adams LJ, Mann C, Davis-Gardner ME, Suthar MS, Shi PY, Saphire EO, Fremont DH, Curiel DT, Alter G, Diamond MS. An intranasal vaccine durably protects against SARS-CoV-2 variants in mice. Cell Rep. 2021;36(4):109452. Epub 20210710. doi: 10.1016/j.celrep.2021.109452. PubMed PMID: 34289385; PMCID: PMC8270739.
37. Gage E, Van Hoeven N, Dubois Cauwelaert N, Larsen SE, Erasmus J, Orr MT, Coler RN. Memory CD4(+) T cells enhance B-cell responses to drifting influenza immunization. Eur J Immunol. 2019;49(2):266-76. Epub 2018/12/15. doi: 10.1002/eji.201847852. PubMed PMID: 30548475; PMCID: PMC6494461.
38. Davenport ML, Sherrill TP, Blackwell TS, Edmonds MD. Perfusion and Inflation of the Mouse Lung for Tumor Histology. J Vis Exp. 2020(162). Epub 20200806. doi: 10.3791/60605. PubMed PMID: 32831298; PMCID: PMC7877253.
39. Schindelin J, Arganda-Carreras I, Frise E, Kaynig V, Longair M, Pietzsch T, Preibisch S, Rueden C, Saalfeld S, Schmid B, Tinevez JY, White DJ, Hartenstein V, Eliceiri K, Tomancak P, Cardona A. Fiji: an open-

source platform for biological-image analysis. Nat Methods. 2012;9(7):676-82. Epub 20120628. doi: 10.1038/nmeth.2019. PubMed PMID: 22743772; PMCID: PMC3855844.

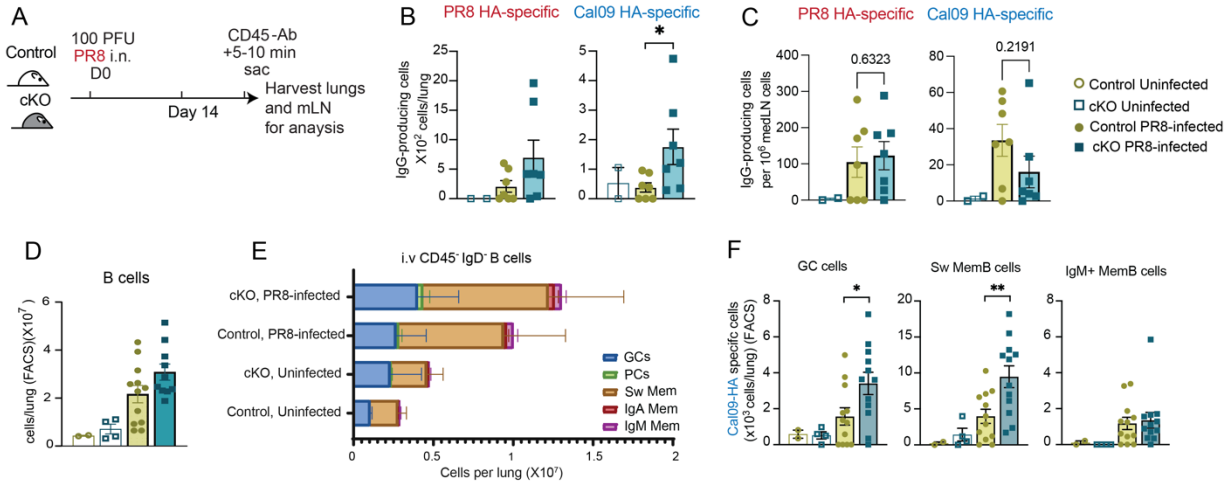

Figure 1. *Generation of cross-reactive B cell responses in the lungs is regulated by B cell αv integrin.* $\alpha v^{+/+}$ $CD19^{Cre+}$ (control) and $\alpha v^{fl/fl}$ $CD19^{Cre+}$ (cKO) mice were infected i.n. with 100 plaque-forming units (PFU) of live PR8 IAV. 14 days later all mice received a retro-orbital (r.o.) injection with 1µg anti-CD45 antibody (Ab) (α-CD45-BUV395) five minutes prior to euthanasia. (**A**) Schematic for experimental procedure. (**B-C**) IgG-secreting cells in the lung **(B)** or mediastinal lymph node (medLN) **(C),** that recognize either PR8-HA or Cal09-HA enumerated by ELISpot. Cells per lung were calculated by multiplying the frequency of live cells by the total number of live lymphocytes counted. **(D)** Flow cytometry analysis and quantification of live cells gated as B cells that are lung-resident cells i.v. $CD45^-$. **(E)** B cells were gated into sub populations based on surface markers. Cells were first gated as live lung-resident cells (i.v. CD45-unlabeled) and Plasma cells (PCs) were gated as IgD- IRF4+ CD138+ cells. B cells were gated as CD19 and CD138 (CD19+ CD138+/-), IgD+ cells were excluded from the analysis, germinal center cells (GCs) were gated as IgD- IRF4- CD138- Fas+ PNA+ and Sw memory B cells were gated as IgD- IRF4- CD138- Fas- PNA- IgM- IgA-. Cells per lung were calculated by multiplying the frequency of each population, as determined by flow cytometry, by the number of total live cells recovered from the tissue harvest. (**F**) Antigen-specific germinal center (GC, left), class-switched memory B cells (Sw Mem B cells, middle) and IgM+ memory B cells (right) from the lung were enumerated by flow cytometry from the i.v. $CD45^-$ population (see Supplemental **Figure 1** for gating strategy). Each dot represents an individual mouse (n= 2-4 mice for uninfected group and n=7-12 mice for infected groups). Data are means ± SEM either representative experiment from 3 independent experiment (**B** and **C**) or the combination (**D - F**) of two independent experiments. *p<0.05, **p<0.01 by Mann-Whitney U-test between the two PR8-infected groups.

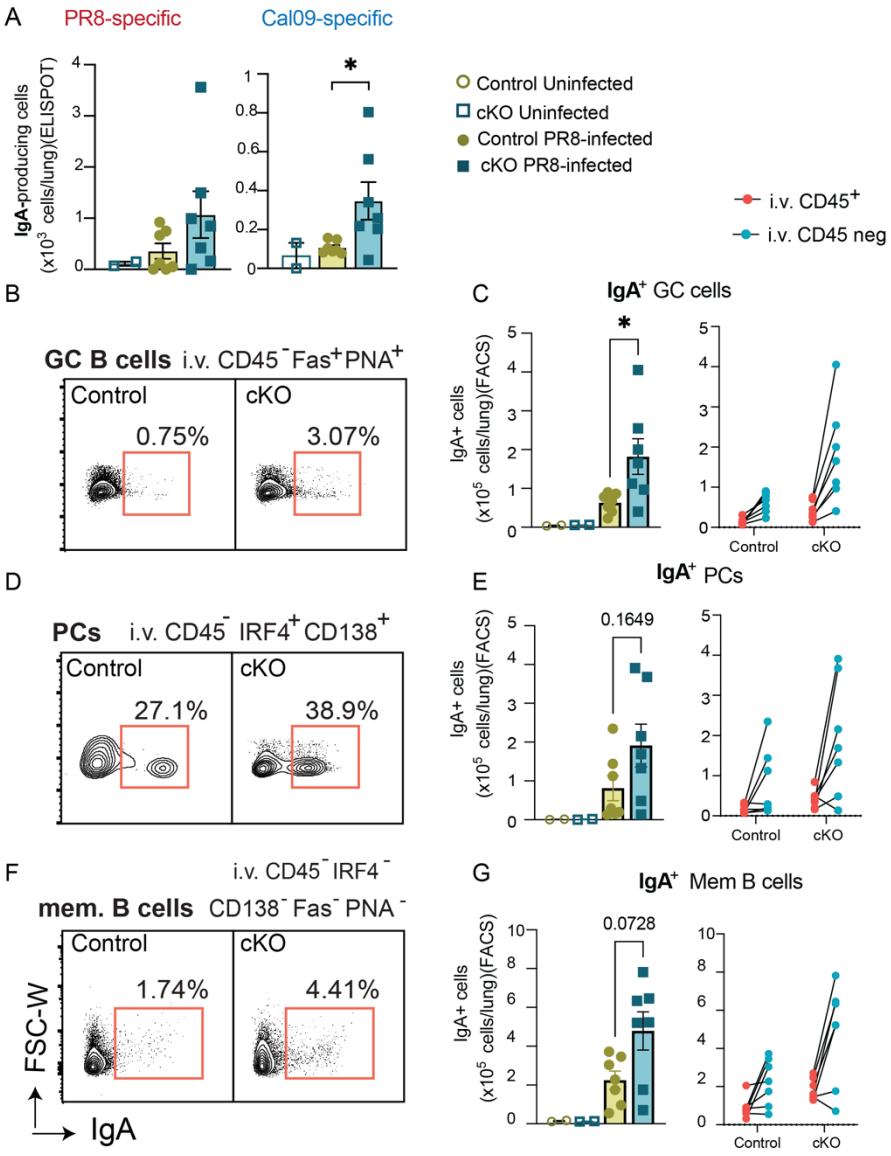

Figure 2. *Absence of B cell αv integrin promotes IgA B cell response in the lungs after influenza infection.* $\alpha v^{+/+}$ $CD19^{Cre+}$ (control) and $\alpha v^{fl/fl}$ $CD19^{Cre+}$ (cKO) mice were infected i.n. with 100 plaque-forming units (PFU) of live H1N1 PR8 IAV. After 14 days of infection all mice received r.o. injection with 1μg α-CD45-BUV395 five minutes prior to euthanasia. (**A**) IgA-secreting cells in the lungs that recognize PR8-HA (left) or Cal09-HA (right) as detected by ELISPOT. Cells per lungs were calculated by multiplying the frequency of live cells by the total number of live lymphocytes counted. (**B-F**) Representative flow plots of the expression of IgA on GC B cells (top), PCs (middle) and mem B cells (bottom) (See Supplemental **Figure 1** for gating strategies) are shown in (**B**) (**D**) and **(F)**. Live lung-resident cells (i.v. CD45-) were gated on CD19 and CD138 to identify B cells (CD19+ CD138+/-), IgD+ cells were excluded from the analysis. Plasma cells (PCs) were gated as IgD- IRF4+ CD138+, germinal center cells (GCs) were gated as IgD- IRF4- CD138- Fas+ PNA+ and IgA memory B cells were gated as IgD- IRF4- CD138- Fas- PNA- IgM- IgA+. Quantification from flow analysis is shown in (**C**) (**E**) and (**G**). Cells per lung for IgA+ GCs (**C**), IgA+ PCs (**E**) and IgA Memory B cells (**G**) is shown in the control and cKO, uninfected and infected mice (left) and the frequency of each population comparing the cell number of resident (CD45-unlabeled) vs circulating (CD45-labeled) cells in the control and cKO mice (right). Each dot represents an individual mouse (n= 2mice for uninfected group and n=6-7 mice for infected groups). Data are means ± SEM from one representative experiment from 3 independent experiments. *p<0.05 by Mann-Whitney U-test between the two PR8-infected groups.

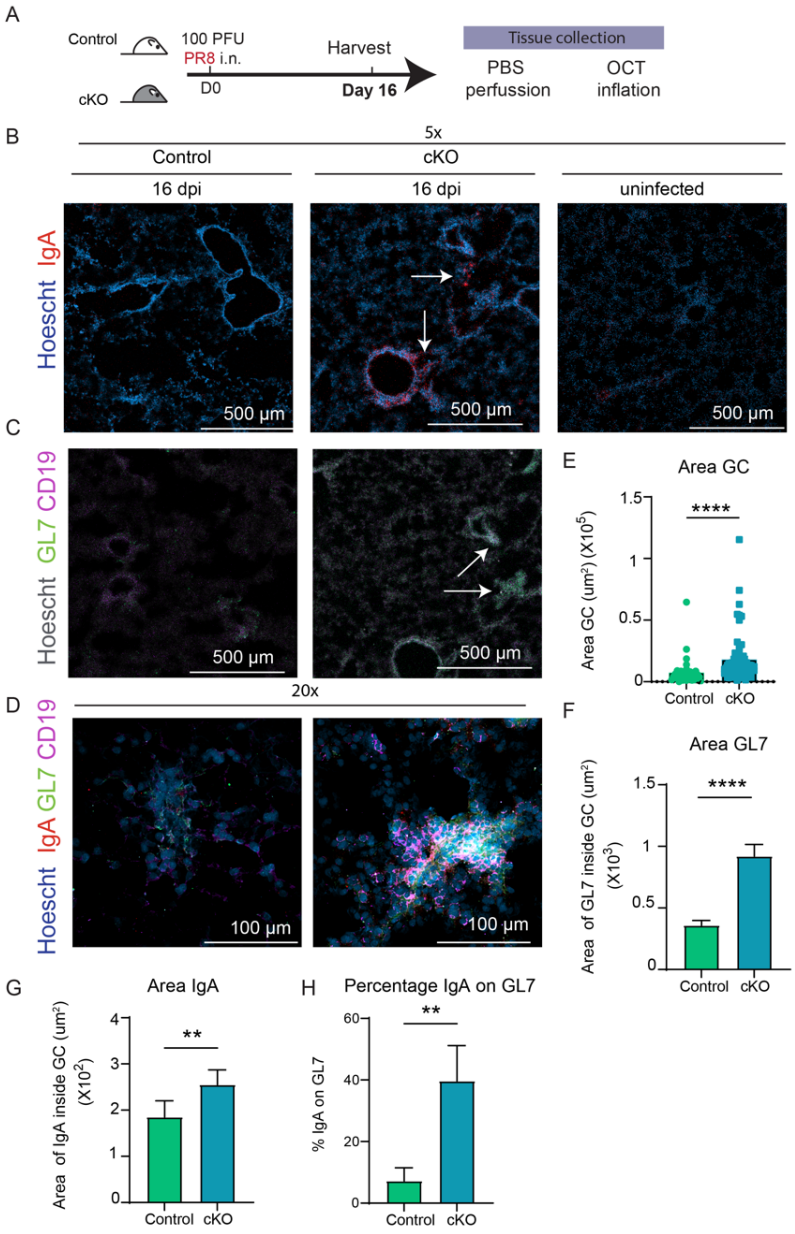

Figure 3. *Loss of B cell αv integrin enhances the induction of iBALT in lungs after viral infection.* $\alpha v^{+/+}$ $CD19^{Cre+}$ (control) and $\alpha v^{fl/fl}$ $CD19^{Cre+}$ (cKO) mice were infected i.n. with 100 plaque-forming units (PFU) of live PR8 IAV. Lungs were harvested after 16 days post infection (dpi). (**A**) Schematic of mice infection and tissue collection for lung tissue staining. (**B-C**) Representative confocal images of lungs from uninfected control mouse and infected control or cKO mice. Images representing one single plane at 5x magnification. Scale bar 500 µm. (**B**) Lung staining for Hoechst (nucleus, Blue) or IgA (red). Airways surrounded by IgA staining are shown by arrows. (**C**) Lung staining for Hoechst (nucleus, gray), GL7 (green), and CD19 (magenta). Arrows represent GL7 positive and CD19 positive structures corresponding to iBALTs. (**D**) Representative confocal images of lungs from control or cKO mice 16 dpi. Images representing one single plane at 20x magnification labeled with Hoechst (nucleus, Blue), IgA (red), GL7 (green), and CD19 (magenta) showing iBALTs. Scale bar 100 µm. (**E**) Scatter plot with a bar graph showing the average size (μm^2) of GL7+CD19+ iBALT structures by manually quantifying the area of these structures. Every dot is the size of 1 iBALT structure (35-65 structures) from 22-28 different fields of sections viewed at 10x from 3 different mice per genotype. (**F and G**) Bar graph showing mean and SEM of the area (μm^2) of (**F**) GL7 and (**G**) IgA positive staining inside the structures (N= 35-65) as defined in **E**. (**H**) Bar graph showing mean and SEM of the percentage of IgA+GL7+ staining within iBALT structures. Sections (N=7-9) viewed at 20x from 3 different mice per group. **p<0.01, ****p<0,0001 by Mann-Whitney U-test.

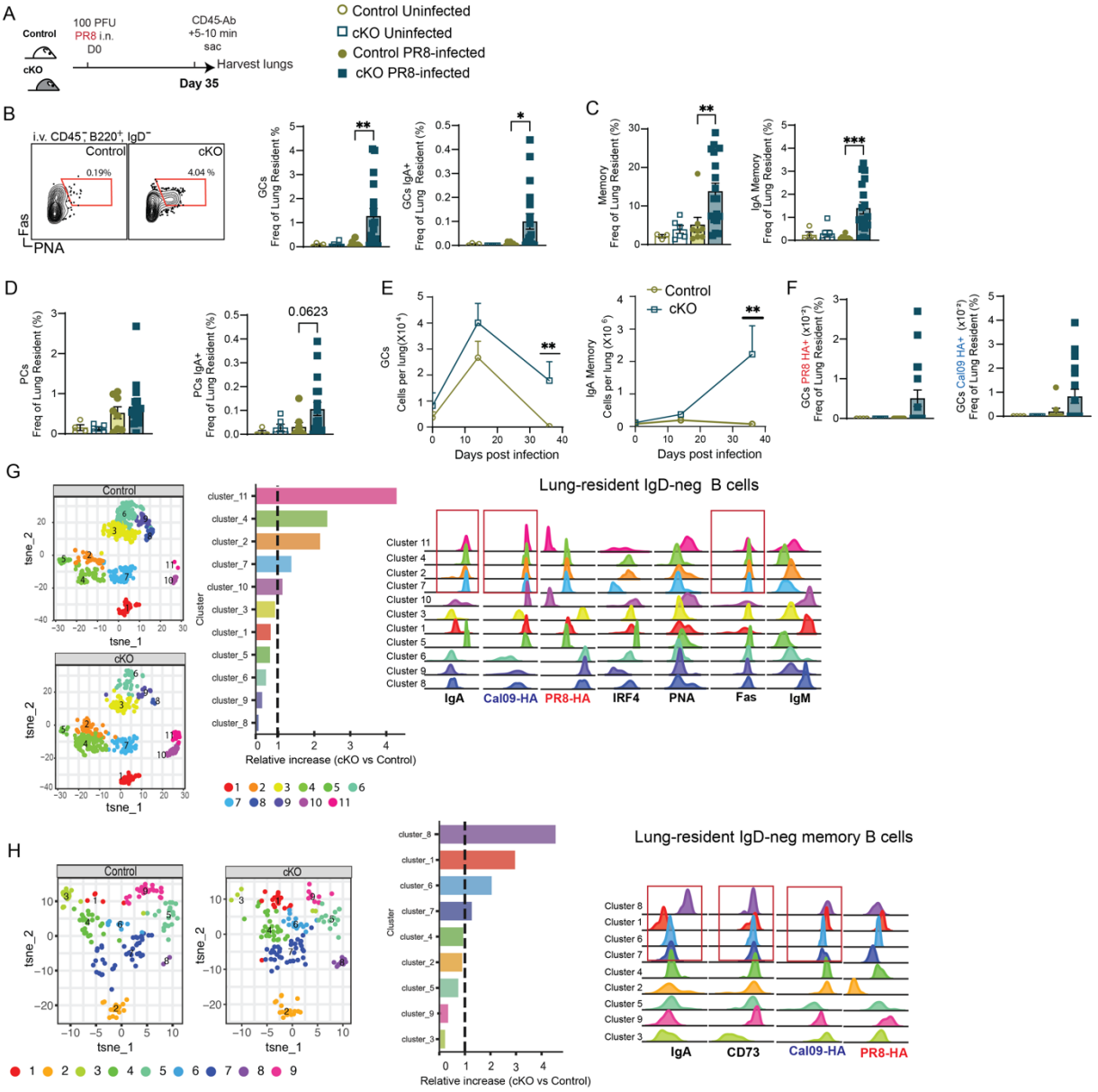

Figure 4. *Absence of B cell αv integrin leads to sustained increase in cross-reactive IgA+ GC and memory B cells in the lungs.* $\alpha v^{+/+}$ $CD19^{Cre+}$ (control) and $\alpha v^{fl/fl}$ $CD19^{Cre+}$ (cKO) mice were infected i.n. with 100 plaque-forming units (PFU) of live PR8 IAV. After 35 days of infection, all mice were injected r.o. with 1μg α-CD45-APC five minutes prior to euthanasia. (**A**) Schematic for experimental procedure. (**B**) Representative flow plot of the lung-resident germinal center cells (GC: B220+ IgD- IRF4- Fas+ PNA+) from a control and cKO mice at 35 days post infection. Bar graph shows the frequency of lung-resident (i.v CD45 negative) GCs, GCs IgA+ cells as determined by flow cytometry. (**C**) Frequency of the lung-resident (i.v CD45-) class-switched (Memory) (B220+ IgD- IRF4- Fas- PNA- IgM-) and IgA+ Memory cells and (**D**) Lung-resident plasma cells (PCs, B220+ IgD- IRF4+) and IgA+ plasma cells, as determined by flow cytometry. Each dot represents an individual mouse (n=3-5 mice for uninfected group and n=6-10 mice for infected groups). Data are mean ± SEM of two representative experiments combined from 4 independent experiments. **p*<0.05, ***p*<0.01, ****p*<0.001 by Mann-Whitney U-test between the two PR8-infected groups. (**E**) Cell per lung for GC B cells or IgA+ memory B cells calculated at day 0 (N= 6 – 9), 14 (N= 9 – 12) and 35 (N= 8 – 18) is shown, ***p*<0.01 by Mann-Whitney U-test between the two PR8-infected groups. (**F**) Frequency of GCs PR8-HA+ and GCs Cal09-HA+ determined by flow cytometry. (**G**) t-SNE plot of HA-specific lung-resident IgD- B cells (i.v CD45- B220+ IRF4+/- IgD- PR8-HA+/Cal09-HA+) from lungs of infected control (top) and cKO

mice (bottom) with the PhenoGraph clusters (left). Fold increase of the cell proportion per cluster in the cKO vs the control mice (middle). Histograms of the expression of the markers included in the analysis for each cluster, red boxes include the clusters with an increased frequency in the cKO mice compared to the control (right). (**H**) Mice were infected i.n. with 100 plaque-forming units (PFU) of live PR8 IAV and re-challenged at day 31 with 50 PFU live PR8. All mice received r.o. injection with 1µg α-CD45-APC five minutes prior to euthanasia. t-SNE plot of lung-resident IgD- memory B cells (iv CD45- B220+ IRF4+/- IgD-, Fas- PNA-) from infected control (left) and cKO mice (right) with the PhenoGraph clusters. Fold increase of the cell proportion per cluster in the cKO vs the control mice (middle). Histograms of the expression of the markers included in the analysis for each cluster, red boxes include the clusters with an increased frequency in the cKO mice compared to the control (right). Analysis is based on n= 6 mice per group in both sets of cluster analysis.

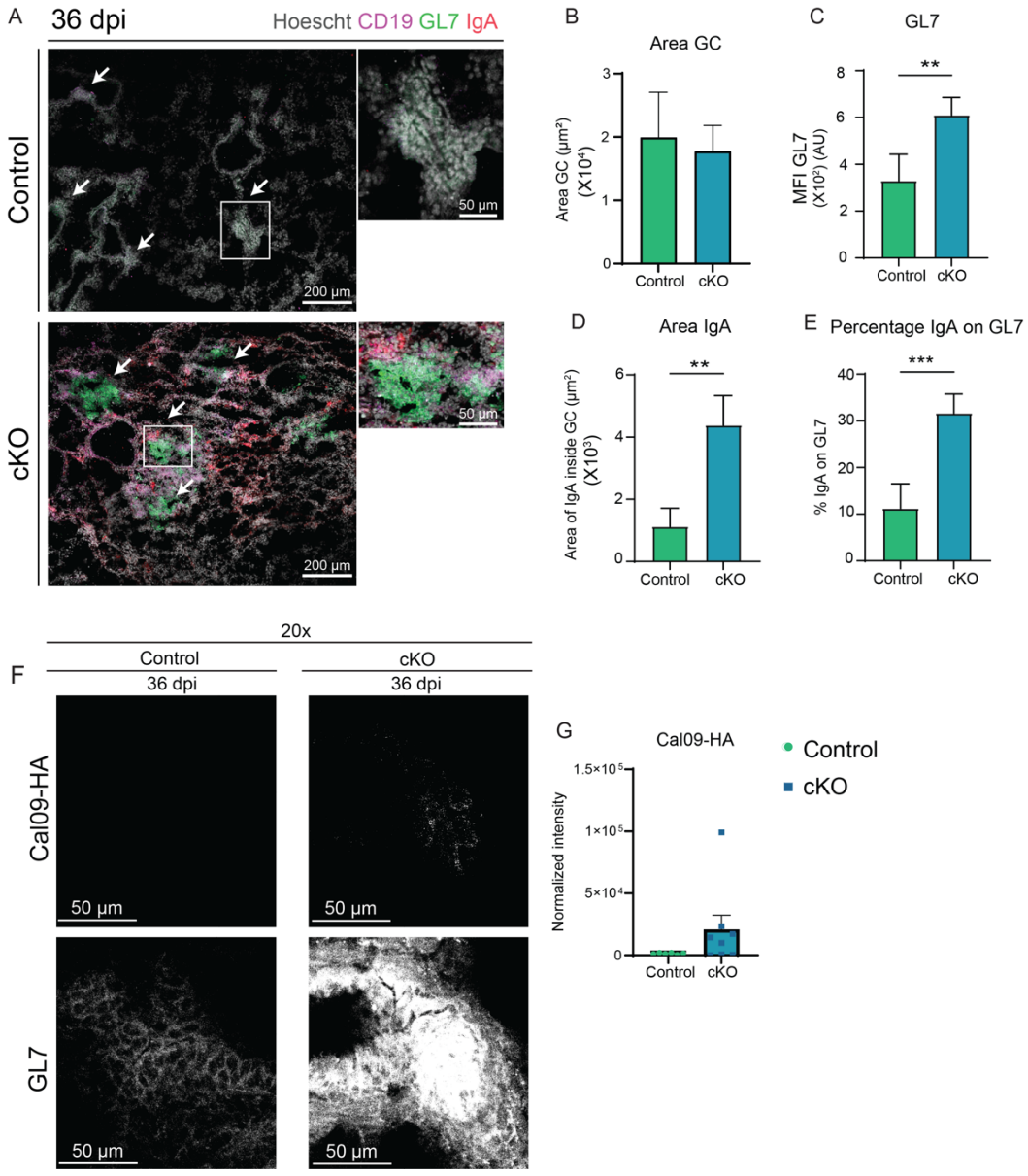

Figure 5*: Absence of αv B cell integrin leads to persistence of GC reactions in the lungs after influenza infection.* $\alpha v^{+/+}$ $CD19^{Cre+}$ (control) and $\alpha v^{fl/fl}$ $CD19^{Cre+}$ (cKO) mice were infected i.n. with 100 plaque-forming units (PFU) of live PR8 IAV. Lungs were harvested after 36 days post infection (dpi). (**A**) Representative confocal images of lung sections of one single plane from infected control (top) and cKO mice (bottom) at 20x magnification, scale bar 200 µm. Lung staining for Hoescht (grey), CD19 (magenta), GL7 (green) and IgA (red). Arrows represent GL7 positive structures corresponding to iBALTs. The insets highlight iBALTs, scale bar 50 µm. (**B – E**) Bar graph showing mean and SEM of the GC area in μm^2 (**B**), GL7 mean fluorescence intensity (MFI) within the iBALT structures (**C**), IgA area inside the GC in μm^2 (**D**) and percentage of IgA staining overlapping with GL7 within the iBALT (**E**). Quantifications made from 9-12 different fields of sections viewed at 10x from 3 different mice per genotype (N= 12-27). (**F**) Representative confocal images of iBALT regions, stained for Cal09-HA (top) and GL7 (bottom) of lungs from infected control (left) and cKO (right) mice at 20x magnification. (**G**) Bar graph of the normalized intensity of Cal09-HA staining from 6 – 8 different fields of sections viewed at 20x from 3 different mice per genotype. **p<0.01, ***p<0.001 by Mann-Whitney U-test.

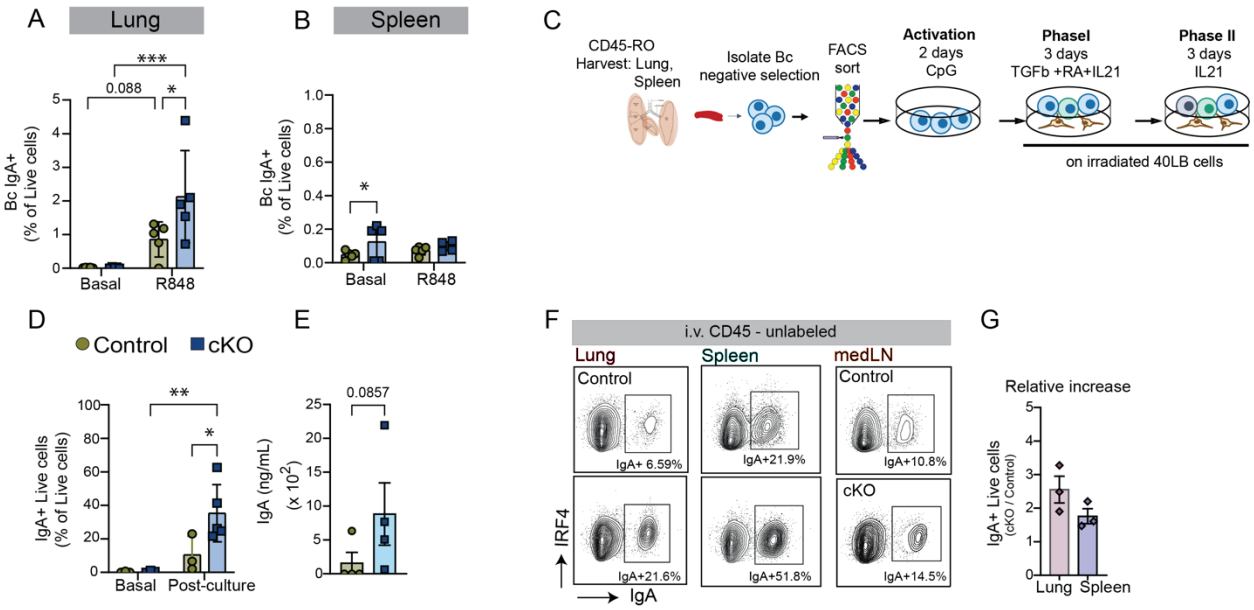

Figure 6: *B cell αv integrin regulates TLR signaling dependent IgA B cell differentiation.* (**A-B**) Frequency of IgA-expressing B cells after 4 days of culture of (**A**) lung and (**B**) spleen B cells with R848 only as determined by flow cytometry. (**C**) Schematic of the experimental procedure. C57BL/6 (control) and $\alpha v^{fl/fl}$ $CD19^{Cre+}$ (cKO) mice were injected r.o. with 1µg α-CD45-APC five minutes prior to euthanasia. Lung, spleen and medLN were then collected and sorted for i.v.CD45-unlabeled resident cells and plated for a total of 8 days. Cells were activated with CpG (1 µg/mL) for 2 days and then added TGFβ (2ng/mL), Retinoic acid (100nM) and IL-21 (40 ng/mL). (**D**) Frequency of IgA-expressing live cells within lung-resident B cells after culture as determined by flow cytometry. (**E**) Secreted IgA as measured by ELISA of the supernatant of lung-resident B cells after TGFβ, RA and IL-21 culture. (**F**) Representative flow plots of lung, spleen and medLN resident B cells after the entire 8-day culture protocol. Cells were gated from live lymphocytes. (**G**) Relative increase in the frequency of IgA+ live cells, in the cKO vs the control cultures comparing cultures from lung and spleen B cells after the 8-day culture protocol. Each dot represents biological replicate from independent experiments. Each dot represents culture with cells from individual mice from one representative experiment shown out of 2 independent experiments. Bar graphs show mean and SEM, *p<0.01, **p<0.001, ***p<0.0001 by Mann-Whitney U-test (**E**) or 2-way ANOVA (**A**, **B** and **D**).